Journal Pre-proofs

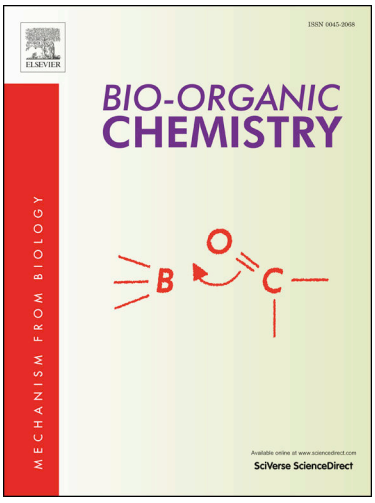

Synthesis and biological evaluations of *N'*-Substituted methylene-4-(quinoline-4-amino) benzoylhydrazides as potential anti-hepatoma agents

Baicun Li, Feifeng Zhu, Fengming He, Qingqing Huang, Tong Wu, Taige Zhao, Yingkun Qiu, Zhen Wu, Yuhua Xue, Meijuan Fang

PII: S0045-2068(19)31970-4
DOI: https://doi.org/10.1016/j.bioorg.2020.103592
Reference: YBIOO 103592

To appear in: *Bioorganic Chemistry*

Received Date: 20 November 2019
Revised Date: 16 January 2020
Accepted Date: 18 January 2020

Please cite this article as: B. Li, F. Zhu, F. He, Q. Huang, T. Wu, T. Zhao, Y. Qiu, Z. Wu, Y. Xue, M. Fang, Synthesis and biological evaluations of *N'*-Substituted methylene-4-(quinoline-4-amino) benzoylhydrazides as potential anti-hepatoma agents, *Bioorganic Chemistry* (2020), doi: https://doi.org/10.1016/j.bioorg.2020.103592

Synthesis and biological evaluations of *N'*-Substituted methylene-4-(quinoline-4-amino) benzoylhydrazides as potential anti-hepatoma agents

Baicun Li,[1, 2, #] Feifeng Zhu,[1, #] Fengming He,[1, #] Qingqing Huang,[1] Tong Wu,[1] Taige Zhao,[1] Yingkun Qiu,[1] Zhen Wu,[1] Yuhua Xue,[1, *] Meijuan Fang[1, *]

1. *Fujian Provincial Key Laboratory of Innovative Drug Target Research and State Key Laboratory of Cellular Stress Biology, School of Pharmaceutical Sciences, Xiamen University, Xiamen 361102, China*
2. *State Key Laboratory of Medical Molecular Biology, Department of Physiology, Institute of Basic Medical Sciences, Chinese Academy of Medical Sciences and School of Basic Medicine, Peking Union Medical College, Beijing 100005, China*

[#]These authors contributed equally to this work.

*Corresponding author. Fujian Provincial Key Laboratory of Innovative Drug Target Research and State Key Laboratory of Cellular Stress Biology, School of Pharmaceutical Sciences, Xiamen University, Xiamen 361102, China

E-mail addresses: fangmj@xmu.edu.cn (M.-J. Fang), xueyuhua@xmu.edu.cn (Y.-H. Xue).

Abstract

In the effort to develop novel quinoline derivatives for the treatment of liver cancer, we synthesized a series of *N'*-Substituted methylene-4-(quinoline-4-amino) benzoylhydrazides and evaluated their biological activities as anticancer agents. Compounds **5h** and **5j** were found to be the potent antiproliferative agents against HepG2 cell line with an IC_{50} value of 12.6±0.1 μM and 27.3±1.7 μM, respectively. The most effective compound **5h** also exhibited potent cytotoxicity against SMMC-7721 and Huh7 cells with IC_{50} values of 9.6±0.7 μM and 6.3±0.2 μM, respectively. Inspiringly, both **5h** and **5j** exhibited lower cytotoxic property in normal cells than hepatic carcinoma cells. Compounds **5h** and **5j** could down-regulate mRNA level of c-Myc and expression level of c-Myc. Meanwhile, they decreased expression level of anti-apoptotic protein Bcl-2 and increased expression levels of pro-apoptotic protein Bax and cleaved PARP with reference to tubulin. So various assays including cell colony formation, cell cycle distribution, as well as cell apoptosis and migration were performed to understand their antitumor role. It was confirmed that **5h** and **5j** inhibited the growth of HepG2 cells due to their anti-survival effect, induction of cell cycle arrest and cell apoptosis, and inhibition of cell migration. These results demonstrated that **5h** might be as potential lead compounds to develop anticancer agents for the treatment of hepatocellular carcinoma.

Keywords: Liver cancer; Methylene-4-(quinoline-4-amino) benzoylhydrazide; Anticancer; c-Myc inhibitor; Apoptosis.

1. Introduction

Cancer is a major public health problem and consumes a lot of social resources[1]. Liver cancer is the fifth most common malignant tumor in the world. The incidence of liver cancer has been increasing all over the world in recent years [2-5]. Hepatocellular carcinoma is the most common type of liver cancer and also is the most common primary malignant tumor of the liver. The morbidity and mortality of hepatocellular carcinoma continued increased in recent years make it urgent. Therefore, it is necessary to speed up the development of the target drugs for hepatocellular carcinoma. C-Myc protein is a transcription factor which targets genes involved in cell growth, cell-cycle progression, transcription, differentiation, apoptosis, and cell motility. Dysregulation of c-Myc is commonly found in many cancer [6-8]. Clinical research has been shown that c-Myc is overexpressed in most hepatocellular carcinoma patients and correlated with poor prognosis [9]. Further down-regulating of c-Myc in HepG2 cells by RNAi could significantly inhibit migration, invasion and proliferation of HepG2 cells. Therefore, c-Myc is thought to be a potential therapeutic target for hepatocellular carcinoma [10].

Quinoline is one of the most ubiquitous heterocycles and appears as an important structural component in many natural products and synthetic compounds that are associated with a wide spectrum of bioactivities such as antifungal [11], antibacterial [12], and anticonvulsant [13]. Quinoline derivatives play an important role in the development of anticancer drugs. For example, camptothecin bearing quinolone motif is the first natural topoisomerase inhibitor with broad-spectrum anti-tumor activity, and it is mainly used for the treatment of colon cancer, ovarian cancer, liver cancer, bone cancer and leukemia [14]. Semisynthetic camptothecin derivatives, such as topotecan and irinotecan, have been approved to treat ovarian and colon cancer, respectively[14]. Neratinib (LNTN) with a quinoline pharmacophore is a double inhibitor of HER2/EGFR, approved as an orally available drug that is used in the extended adjuvant therapy of early-stage breast cancer [15]. Besides, 8-hydroxyquinoline and its

derivatives isolated from the phytotoxic activity of *T. chinensis* roots [16], exhibit a relatively promising anticancer effect in vitro and in vivo, being reported as potential anti-tumor agent [17]. 83b1 is a novel quinoline derivative which can inhibit cancer growth in human esophageal squamous cell carcinoma (ESCC) [18]. Additionally, William Kemnitzer *et al.* identified a series of 1-benzoyl-3-cyanopyrrolo [1,2-a] quinoline derivatives that are more active in human breast cancer cell line T47D, human colon cancer cell HCT116 and hepatocellular carcinoma cell line SNU398 [19].

To develop new type quinoline derivatives for the treatment of hepatocellular carcinoma, we first synthesized a series of *N'*-Substituted methylene-4-(quinoline-4-amino) benzoylhydrazides and evaluated their antiproliferative activities against HepG2 cells using MTT assay. Compounds **5h** and **5j** demonstrated more potent inhibiting activity against HepG2 cells compared with other synthesized compounds. In vitro cell cytotoxicity of **5h** and **5j** was then investigated against the other two hepatocellular carcinoma cell lines (SMMC-7721 and Huh7) and normal cell lines (LO2 and MRC-5) by MTT assay using Neratinib (LNTN) as a positive control. Subsequently, **5h** and **5j** as representative compounds were examined for their effects on alterations in the expression of oncogene c-Myc and apoptotic proteins, representing Bcl-2, Bax, as well as cleaved PARP. Additionally, further experiments into an antitumor role behind the antitumor activity of compounds **5h** and **5j** were also carried out, including cell colony formation, cell cycle progression, apoptotic induction, and cell migration. Taken together, we found quinoline derivatives **5h** might be as potential lead compounds to develop anticancer agents for the treatment of hepatocellular carcinoma.

2. Results and discussion

2.1. Chemistry

The synthesis of *N'*-Substituted methylene-4-(quinoline-4-amino) benzoylhydrazides (**5a-5p**) were delineated in **Scheme 1**. 4-Hydroxyquinoline (**1**) was

firstly halogenated to form 4--chloroquinoline (**2**) using phosphorus oxychloride[20]. Ethyl 4-(quinolin-4-ylamino) benzoate (**3**) was then prepared from benzocaine by *N*-alkylation using 4--chloroquinoline (**2**) in the presence of hydrochloric acid as a catalyst in refluxing butyl alcohol. Compound **3** was treated with hydrazine hydrate in refluxing ethanol, followed by condensation with different substituted aldehydes to give the corresponding target compounds **5a-5p** in 49−92% yields after isolation.

All new target compounds were characterized by proton nuclear magnetic resonance (^{1}H NMR), carbon nuclear magnetic resonance (^{13}C NMR), and electrospray ionization mass spectrometry (ESI-MS). The C=N double bonds of *N*-acylhydrazones were in the E form based on reported studies [21-24]. Furthermore, a single E geometrical isomer of the representative compound **5j** was identified by H-9 (-NH-) signal observed as a single peak (δ 10.46, H-9) in ^{1}H NMR spectra and the cross-peak (10.46, 8.62) intensities of -CONH- and =CH-(H-9/H-22) observed in 2D NOESY spectrum (**Figure S4**, see Supporting Information). Therefore, we concluded that the stereochemistry of compounds **5a-5p** as a single E geometrical isomer.

Insert Scheme 1 here.

Scheme 1. Preparation of target compounds **5a-5p**

2.2. Biological evaluation

*2.2.1. In vitro cytotoxic activity of the target compounds **5a-5p** against HepG2 cells*

The synthesized compounds were evaluated for their cytotoxic activity against HepG2 cells by MTT assay using Neratinib (LNTN) as a positive control. The cytotoxic activity of compounds against HepG2 cells was first tested at the concentration of 25 μM (Figure S1). As shown in **Figure S1**, most target compounds showed very weak cytotoxic activity (<50%) against HepG2 cells at the concentration of 25 μM, while **5h** and **5j** displayed significant inhibitory effect (100% and 90.70%, respectively) on the

proliferation of HepG2 cells at the same tested concentration. To clarify the effect of different substitutions (R) on the cytotoxic activity, the IC_{50} values of these compounds for the cytotoxic activity against HepG2 cells were further determined and listed in **Table 1**. Considering the IC_{50} results in HepG2 cells, we attempted to establish the structure-activity relationship (SAR) among the tested compounds. Firstly, we found that alkyl substitutions (**5a** & **5b**) at nitrogen atom (N') of *N*-acylhydrazone had little effect on the cytotoxic activity. However, different substituted groups of the phenyl ring introduced at the *N*′-methylene position displayed an important relationship with cytotoxic activity. Compounds **5d**, **5e**, and **5k** possessing carboxyl (COOH) or nitro (NO_2) group at phenyl ring were inactive. Compound **5l** which had 3,5-dibromo and 4-hydroxyl groups at phenyl ring significantly decreased cellular cytotoxic activity. However, except compound **5i**, three compounds (**5g**, **5h**, and **5j**) with 2 hydroxy (OH) or Methoxy (OCH_3) substitutions at phenyl enhanced cytotoxic activity. Compared with compound **4**, the introduction of aromatic heterocycles at the N′- methylene (**5m**, **5n**, **5o**, and **5p**) was unhelpful for cytotoxic activity. Above all, **5h** and **5j** displayed better inhibition against HepG2 cells than the other synthesized compounds.

Insert Table 1 here.

Table 1. *In vitro* cytotoxic activity of the target compounds **5a**-**5p** against HepG2 cells

Both anti-hepatoma effect and safety of **5h** and **5j** were further determined by MTT assay *in vitro*. Three different human hepatic carcinoma cell lines such as HepG2, SMMC-7721, and Huh7 were used to evaluate the anti-hepatoma effect of these two selected compounds. Meanwhile, the safety of two selected compounds toward normal cells such as LO2 and MRC-5 was evaluated. The activities of **5h**, **5j**, and the reference drug Neratinib (LNTN) were shown in Table 2. As shown in Table 2, **5h** exerted superior antiproliferative effects against HepG2, SMMC-7721, and Huh7 cell lines, while **5j** had lower antitumor activity in all three cancer cell lines compared to **5h**,

especially SMMC-7721. Inspiringly, both **5h** and **5j** exhibited lower cytotoxic property in normal cells than hepatic carcinoma cells. So compounds **5h** and **5j** were selected for further study in more detail.

Insert Table 2 here.

Table 2. The anti-hepatoma effect and safety of **5h** and **5j**

*2.2.2 Modulating effect of **5h** and **5j** on the key proteins of cancer*

Inhibition of the expression of oncogene c-Myc. c-Myc plays an important role in tumorigenesis and the development of cancer, being a potential therapeutic target for hepatocellular carcinoma. So the represented compounds **5h** and **5j** were first evaluated their regulating effect on the proto-oncogene c-Myc. As shown in **Figure 1A**, the expression of protein c-Myc was significantly inhibited by 15 μM **5h** and 20 μM **5j**. We also detected that the expression of the c-Myc oncogene mRNA was inhibited by compounds **5h** and **5j** (**Figure 1B**), especially **5h**. It suggests that compounds **5h** and **5j** may inhibit cell proliferation and induce cell cycle arrest and eventual apoptosis.

Regulation of apoptosis-related protein expression. The BCL-2 protein family having pro-apoptotic (*e.g.* Bax) and anti-apoptotic proteins (*e.g.* Bcl-2) are crucial for the regulation cell apoptosis, tumorigenesis and cellular responses. So we checked the levels of anti-apoptotic protein Bcl-2 and pro-apoptotic protein Bax in HepG2 cells treated with or without compounds **5h** and **5j**. The expression of Bcl-2 and Bax proteins was first determined by Western Blotting analysis. Treatment of HepG2 cells with compound **5h** and **5j** resulted in the down-regulation of anti-apoptotic protein Bcl-2 levels and the up-regulation of the pro-apoptotic protein Bax (**Figure 1C**, visually represented by grayscale analysis). Meanwhile, the mRNA levels of Bcl-2 and Bax were examined using qRT-PCR. The results showed that anti-apoptotic protein Bcl-2 decreased, while pro-apoptotic protein Bax increased after **5h** or **5j** treatment (**Figure**

1D). It was consistent with Western Blotting analysis. Next, the immunofluorescence assay (**Figure 1E)** showed that Bax in the cytoplasm significantly increased after **5h** treatment at indicated doses, whereas there is a little increase after **5j** treatment at indicated doses. All the above results imply that **5h** and **5j** may induce apoptosis of HepG2 cells through mitochondrial apoptosis. Moreover, the increase in cleaved PARP (c-PARP, a marker for apoptosis) following treatment of cells by **5h** and **5j** indicates cell death via apoptosis (**Figure 1C**).

Insert Figure 1 here.

Figure 1. Modulating effect of **5h** and **5j** on the key proteins of cancer. (A). The expression level of c-MYC in HepG2 cells treated with **5h** or **5j** for 24 h, determined via Western blot. (B). mRNA level of c-MYC in HepG2 cells treated with **5h** or **5j** for 24 h determined by RT-PCR. (C). The expression level of Bcl-2, Bax, and c-PARP proteins in HepG2 cells treated with **5h** or **5j**, determined via Western blot. (D). mRNA levels of Bcl-2 and Bax in HepG2 cells treated with **5h** or **5j** for 24 h determined by RT-PCR. (E). Immunofluorometric images of Bax, DAPI staining and merge in untreated or treated HepG2 cells with **5h** and **5j** for 24 h. (∗) $P < 0.05$, (∗∗) $P < 0.01$, (∗∗∗) $P < 0.001$ compared with control group.

*2.2.3 Anticancer activity of **5h** and **5j** in HepG2*

Anticancer drugs usually target oncogenes and inhibit the growth of tumor cells by regulating cell cycle, apoptosis, and cell migration to achieve the anticancer effect. To confirm the anticancer activity and explore the anticancer role of **5h** and **5j**, we first evaluated their anti-survival effect on HepG2 cells using colony formation assays and examined their cell cycle effect. Then, we studied whether **5h** and **5j** also induced cellular apoptosis to produce an antitumor effect. At last, wound healing assay was carried out to examine whether they reduced the migratory capability of cancer cells.

Colony formation analysis. Colony formation assays for compounds **5h** and **5j** (two

C-Myc inhibitors) were carried out to evaluate their influence on the cancer cell survival and proliferation abilities. As shown in **Figure 2A**, the colonies formed by HepG2 cells were reduced on exposure to **5h** or **5j** at indicated doses. Comparing to **5j**, **5h** has better efficacies against HepG2 cells. It indicates that compound **5h** has a strong anti-survival effect on liver cancer cells.

Cell cycle analysis. Since c-Myc inhibitors may induce cell cycle arrest and eventual apoptosis, the effect of **5h** and **5j** on cell cycle progression using propidiumiodide (PI) staining in HepG2 cells was examined. As illustrated in **Figure 2B**, the G2/M phase cell cycle arrest was significantly increased with HepG2 cells treated with **5h** compared with the control group. When HepG2 cells were treated with **5h** at concentrations of 7.5 and 15 μM for 24 h of incubation, the percentage of cells in the G2/M phase dose-dependently increased from 22.58% to 37.77%. While the incubation of HepG2 cells with increasing concentrations of **5j** (10 and 20 μM) only increased the percentage of cells in the G2/M phase from 22.65% to 27.58% compared to the control cells incubated with DMSO (18.56%). It implies that **5h** has a better cell cycle arrest effect on HepG2 cells than **5j**.

Insert Figure 2 here.

Figure 2. Cell colony formation and cell cycle phase distribution of HepG2 cells with or without treatment of compounds **5h** and **5j**. (A) Compounds **5h** or **5j** suppressed cell colony formation of HepG2 cells. HepG2 cells were incubated with varying concentrations of compounds **5h** or **5j** for 7 days and dyed with 0.1% crystal violet. (B) Compounds **5h** or **5j** induced cell cycle arrest at the G2/M phase in HepG2 cells. HepG2 cells were plated in six-well plates for 24 h and treated with or without compound **5h** and **5j** and at different concentrations for 24 h of incubation. Then, the cells were harvested to determine the PI-stained DNA content via flow cytometry.

Cell apoptosis analysis. According to the above-mentioned apoptosis-related

proteins expression and cell cycle analysis, we supposed that compounds **5h** and **5j** might prime the mitochondria for cytochrome-c release and promote the induction of apoptosis. To confirm their effects on apoptotic induction, HepG2 cells were treated with **5h** or **5j** at different concentrations (5, 10, and 15 μM) for 24 h, and then, the cells were harvested and doubly stained with annexin V/PI (propidium iodide). As shown in **Figure 3**, at the 5 μM concentration **5h** causes 11.15% apoptotic cells, and the percentage increases to 19.65% at 10 μM and 42.6% at 15 μM. Meanwhile, **5j** also displayed a clear dose-dependent apoptotic effect in HepG2 cells, with the percentages of apoptosis cells increasing from 13.09 at 5 μM up to 85.7% at 20 μM. These results confirmed that compound **5h** and **5j** effectively induced cell apoptosis in HepG2 cells in a dose-dependent manner.

Insert Figure 3 here.

Figure 3. Apoptosis analysis of **5h** and **5j** in HepG2 cells. Cells were treated with **5h** or **5j** at distinct concentrations for 24 h, and the cell apoptosis induction of these cells was analyzed by flow cytometry.

Cell migration analysis. Cell migration is a key feature of cancer progression and metastasis and a good anticancer should suppress cell migration. So we also examined whether **5h** and **5j** can inhibit the migration of HepG2 cancer cells at the different concentrations using a wound-healing assay. As shown in **Figure 4A**, **5h** inhibited the migration of the HepG2 cells in a dose-dependent manner. Compound **5f** also reduces the migratory capability of the HepG2 cells as evident from the wound healing assays (**Figure 4B**).

Insert Figure 4 here.

Figure 4. The effects of compounds **5h** and **5j** on the migration of HepG2 cells (A&B). Compounds **5h (A) and 5j (B)** suppressed the migration of HepG2 cells in a dose-dependent

manner.

3. Conclusion

In present work, new *N*'-substituted methylene-4-(quinoline-4-amino) benzoylhydrazide derivatives were synthesized as anticancer agents. These derivatives were initially evaluated for their antiproliferative activities against HepG2 cells. Compounds **5h** and **5j** exhibited higher antiproliferative activities towards HepG2 cells with IC_{50} values of 12.6±0.1 μM and 27.3±1.1 μM, respectively. Compound **5h** also exhibited potent antiproliferative activity with the IC_{50} values of lower than 10 μM against SMMC-7721 and Huh7cells (two human hepatic carcinoma cell lines). Remarkably, **5h** and **5j** lower cytotoxic properties in normal cells. Further bioassays revealed that **5h** and **5j** were found to be two c-Myc inhibitors and could induce the down-regulation of anti-apoptotic protein Bcl-2 and the up-regulation of the pro-apoptotic protein Bax. The antitumor effects of **5h** and **5j** in HepG2 cells resulted from anti-survival effects, cell cycle arrest, the induction of apoptotic cell death, and inhibition of cell migration.

4. Experimental section

4.1. Chemistry

All reagents and solvents were purchased from commercial sources and were used without further purification unless otherwise indicated. All reactions were magnetically stirred and monitored by thin-layer chromatography (TLC) on (Qingdao Haiyang Chemical, China) silica gel 60F-254 by fluorescence. The target compounds were purified by silica gel column chromatography. Melting points (mp) were determined using a Shanghai Jingke SGW X-4 microscope melting point apparatus and were uncorrected. ^{1}H-NMR, ^{13}C-NMR, and NOE spectra were obtained using a Bruker AV2 600 Ultra shield spectrometer, at 600 MHz for ^{1}H NMR and 150 MHz for ^{13}C NMR. Chemical shifts were given in ppm (δ) relative to tetramethylsilane (TMS) as an internal

standard. Splitting patterns are designated as follows: s (singlet), br. s (broad singlet), d (doublet), t (triplet), q (quartet), dd (double doublet), m (multiplet). Mass spectra were measured on a Single Quadrupole Mass Spectrometer (Shimadzu, LCMS-2020). The purities of synthesized compounds were detected by high performance liquid chromatography (HPLC) with a COSMOSIL $5C_{18}$-MS-II column (4.6 ID x 250 mm). The HPLC analysis was performed on an Agilent Technologies 1100 Series HPLC system. The mobile phase was water (A) and acetonitrile (B) in a linear gradient mode as follows: (A) from 95% to 0% and (B) from 5% to 100% during 0-30 min. The flow rate was 1 mL min^{-1}, and the detection wavelengths were 254 nm and 365 nm.

*4.1.1. The synthesis of 4-chloroquinoline (**2**)*

A mixture of 4-hydroxyquinoline **1** (2.90 g, 0.020 mol) and phosphorus oxychloride (30 mL) was stirred at 120℃ for 12 hours. Then, the mixture was cooled to room temperature and the solvent was removed by reduced pressure distillation. The residue was dissolved in 50 mL of code water, the aqueous was adjusted pH to 8-9 with 10% NaOH under cooling in an ice-water bath, and extracted with dichloromethane (DCM, 3 x 30mL). The combined organic layer was dried over anhydrous $MgSO_4$, filtered, and concentrated in vacuo to get the colorless liquid (2.80 g, 87%). ^{1}H NMR (600 MHz, DMSO-d_6): δ 8.87-8.92 (m, 1H), 8.22-8.25 (m, 1H), 8.13-8.17 (m, 1H), 7.91-7.94 (m, 1H), 7.80-7.84 (m, 2H); ESI-MS: positive mode *m/z* 164.3 $[M+H]^+$.

*4.1.2. The synthesis of ethyl 4-(quinolin-4-ylamino)benzoate (**3**)*

4-chloroquinoline **2** (1.60 g, 0.010 mol), benzocaine (1.70 g, 0.010 mol), *n*-butanol (35 mL), and 2 drops of concentrated hydrochloric acid were added to the dry 100 mL round bottom flask, and the reaction mixture was stirred at reflux for 15 hours. Then, the mixture was cooled to room temperature and the resulting solid was filtered off, washed with Hexane, and dried to give a yellowish solid with a yield of 81%. ^{1}H NMR (600 MHz, DMSO-d_6): δ 11.20(s, 1H), 8.88-8.93 (m, 1H), 8.59-8.62 (m, 1H), 8.14-8.17 (m, 1H), 8.10-8.14 (m, 2H), 8.04-8.08 (m, 1H), 7.81-7.85 (m, 1H), 7.67-7.71 (m, 2H), 7.06-7.10 (m, 1H), 4.33-4.39 (m, 2H), 1.33-1.38 (m, 3H); ^{13}C NMR (151 MHz, DMSO-d_6): δ 165.5, 154.7, 143.5, 142.4, 138.8, 134.5, 131.3(2C), 128.3, 127.8, 125.1(2C),

124.4, 120.8, 118.1, 101.2, 61.4, 14.7. ESI-MS: positive mode *m/z* 293.1 $[M+H]^+$.

*4.1.3. The synthesis of 4-(quinolin-4-ylamino) benzohydrazide (**4**)*

A suspension of ethyl 4-(quinolin-4-ylamino)benzoate **3** (2.90 g, 0.010 mol) and hydrazine hydrate (20 mL) in ethanol (15 mL) was stirred and refluxed for 24 h. The reaction mixture was then cooled to room temperature, and the resulting solid was filtered, washed with water, and dried. White solid (2.20 g, 78%); HPLC purity: 99.23%; mp: 272-274℃. ^{1}H NMR (600 MHz, DMSO-d6): δ 9.70 (s, 1H), 9.16 (s, 1H), 8.56 (d, *J*=5.1Hz, 1H), 8.36-8.39 (m, 1H), 7.90-7.95 (m, 1H), 7.87-7.90 (m, 2H), 7.73 (dt, *J*=1.1, 7.6 Hz, 1H), 7.55-7.59 (m, 1H), 7.42 (d, *J*=8.6 Hz, 2H), 7.16 (d, *J*=5.1 Hz, 1H), 4.48 (br. s, 2H); ^{13}C NMR (151 MHz, DMSO-d6): δ 166.0, 151.2, 149.5, 146.9, 144.3, 129.9, 129.7, 128.8(2C), 127.7, 125.4, 122.7, 120.8, 120.3(2C), 103.9. ESI-MS: positive mode *m/z* 279.1 $[M+H]^+$, 301.1 $[M+Na]^+$; negative mode *m/z* 277.1 $[M-H]^-$.

*4.1.4. General procedure for the synthesis of compounds **5a-5p***

A mixture of the appropriate substituted aldehydes (0.2 mol) and 4-(quinolin-4-ylamino) benzohydrazide **4** (55.0 mg, 0.2 mmol) in absolute ethanol (5 mL) containing two drops of trifluoroacetic acid was stirred and refluxed for 8h. Then, the reaction mixture was cooled to room temperature, and the solvent was removed by reduced pressure distillation. The residue was purified by column chromatography (DCM/MeOH/Triethylamine, 200:10:1 (*v/v/v*)) to get (*E*)-*N'*-Substituted methylene-4-(Quinoline-4-Amino) benzoylhydrazides **5a-5p**.

*4.1.4.1. (E)-N'-((1H-imidazol-2-yl)methylene)-4-(quinolin-4-ylamino)benzohydrazide (**5a**)*

According to the general procedure, compound **5a** was obtained by using acetaldehyde. Grey solid; yield 50%; HPLC purity: 96.98%; mp: 279-281℃. ^{1}H NMR (600 MHz, DMSO-d_6): δ 11.80 (br. s, 1H), 9.84 (br. s, 1H), 8.57 (d, *J*=5.7 Hz, 1H), 7.97-8.00 (m, 2H), 7.91-7.93 (m, 1H), 7.77-7.85 (m, 2H), 7.58-7.67 (m, 2H), 7.52 (d, *J*=8.4 Hz, 2H), 7.14 (d, *J*=5.5 Hz, 1H), 1.96 (d, *J*=5.5 Hz, 3H). ^{13}C NMR (151 MHz, DMSO-d_6): δ 162.9, 149.1, 147.0, 144.1, 131.1, 131.0, 129.6, 128.8, 128.1, 127.5, 125.9, 123.5, 121.6, 121.2, 121.2, 120.3, 103.4, 18.9. ESI-MS: positive mode *m/z* 305.1

$[M+H]^+$, 327.1 $[M+Na]^+$, 609.3 $[2M+H]^+$, 631.1 $[2M+Na]^+$; negative mode *m/z* 303.1 $[M-H]^-$.

*4.1.4.2. (E)-N'-butylidene-4-(quinolin-4-ylamino)benzohydrazide (**5b**)*

According to the general procedure, compound **5b** was obtained by using butyraldehyde. Yellowish solid; yield 92%; HPLC purity: 95.53%; mp 147-149 ℃. ^{1}H NMR (600 MHz, DMSO-d_6): δ 11.57 (br. s., 1H), 8.69 (d, *J* = 8.4Hz, 1H), 8.60-8.64 (m, 1H), 8.02-8.06 (m, 4H), 7.76-7.84 (m, 2H), 7.59-7.63 (m, 2H), 7.03 (d, *J* = 6.8 Hz, 1H), 2.21-2.30 (m, 2H), 1.49-1.59 (m, 2H), 0.94 (t, *J* = 1.0 Hz, 3H). ^{13}C NMR (151 MHz, DMSO-d_6): δ 162.4, 152.9, 144.8, 141.3, 133.9, 131.7, 129.7, 129.1, 127.5, 124.5, 124.4, 123.7, 122.2, 118.3, 101.3, 34.4, 19.9, 14.1. ESI-MS: positive mode *m/z* 333.2 $[M+H]^+$, 355.1 $[M+Na]^+$, 687.2 $[2M+Na]^+$.

*4.1.4.3. (E)-4-(quinolin-4-ylamino)-N'-(2-(trifluoromethyl)benzylidene) benzohydrazide (**5c**)*

According to the general procedure, compound **5c** was obtained by using 2-(trifluoromethyl)benzaldehyde. Yellowish solid; yield 77%; HPLC purity: 98.37%; mp: 214-216 ℃. ^{1}H NMR (600 MHz, DMSO-d_6): δ 12.26 (br. s, 1H), 8.89 (br. s, 1H), 8.63 (d, *J* = 6.1 Hz, 1H), 8.57 (d, *J* = 8.4 Hz, 1H), 8.27 (d, *J* = 7.2 Hz, 1H), 8.09 (d, *J* = 7.9 Hz, 2H), 8.01 (d, *J* = 8.3 Hz, 1H), 7.92 (t, *J* = 7.6 Hz, 1H), 7.83 (d, *J* = 7.2 Hz, 1H), 7.76-7.82 (m, 1H), 7.71-7.76 (m, 1H), 7.66 (t, *J* = 7.2 Hz, 1H), 7.60 (d, *J* = 8.6 Hz, 2H), 7.16 (d, *J* = 6.1 Hz, 1H). ^{13}C NMR (151 MHz, DMSO-d_6): δ 163.0, 147.5, 143.3, 143.0, 133.3, 133.1, 132.7, 132.3, 130.5, 130.1, 129.9, 129.2, 127.3, 127.1, 126.7, 126.4, 126.4, 125.6, 125.3, 123.8, 123.4, 122.5, 119.5, 102.7. ESI-MS: positive mode *m/z* 435.1 $[M+H]^+$, 457.1$[M+Na]^+$, 891.2 $[2M+Na]^+$.

*4.1.4.4. (E)-2-((2-(4-(quinolin-4-ylamino)benzoyl)hydrazineylidene)methyl)benzoic acid (**5d**)*

According to the general procedure, compound **5d** was obtained by using 2-formylbenzoic acid. Yellow solid; yield 75%; HPLC purity: 97.94%; mp: 227-229℃. ^{1}H NMR (600 MHz, DMSO-d_6): δ 12.12 (br. s, 1H), 10.17 (br. s, 1H), 9.24 (br. s, 1H), 8.60-8.65 (m, 1H), 8.57 (d, *J*=8.4 Hz, 1H), 8.03-8.21 (m, 3H), 8.00 (d, *J*=8.3 Hz, 1H),

7.89-7.96 (m, 2H), 7.70-7.75 (m, 1H), 7.62-7.69 (m, 1H), 7.51-7.61 (m, 3H), 7.14 (d, *J*=6.1 Hz, 1H). ^{13}C NMR (151 MHz, DMSO-d_6): δ 168.6, 163.1, 150.9, 147.4, 147.0, 144.1, 143.0, 135.1, 132.4(2C), 131.3, 130.8, 130.1, 129.9(2C), 129.6, 127.1, 126.7, 125.3, 123.3, 122.5(2C), 119.4, 102.7. ESI-MS: positive mode *m/z* 411.1 $[M+H]^+$, 433.1 $[M+Na]^+$; negative mode *m/z* 409.0 $[M-H]^-$.

*4.1.4.5. (E)-3-((2-(4-(quinolin-4-ylamino)benzoyl)hydrazineylidene)methyl)benzoic acid (**5e**)*

According to the general procedure, compound **5e** was obtained by using 3-formylbenzoic acid. Yellow solid; yield 74%; HPLC purity: 96.63%; mp: 236-238℃. ^{1}H NMR (600 MHz, DMSO-d_6): δ 12.08 (s, 1H), 10.56 (br. s, 1H), 8.60-8.68 (m, 2H), 8.56 (s, 1H), 8.35 (br. s, 1H), 8.06-8.15 (m, 2H), 7.95-8.04 (m, 4H), 7.75-7.84 (m, 1H), 7.59-7.67 (m, 3H), 7.10 (d, *J*=6.4 Hz, 1H). ^{13}C NMR (151 MHz, DMSO-d_6): δ 167.4, 162.9, 152.8, 147.3, 145.7, 142.1, 141.6, 135.3, 133.4, 132.0, 131.9, 131.1, 130.7, 129.9(2C), 129.8, 127.8, 127.2, 123.8(2C), 123.6, 123.3, 118.8, 101.8. ESI-MS: positive mode *m/z* 411.1 $[M+H]^+$, 433.1$[M+Na]^+$; negative mode *m/z* 409.0 $[M-H]^-$.

*4.1.4.6. (E)-4-((2-(4-(quinolin-4-ylamino)benzoyl)hydrazineylidene)methyl)phenyl acetate (**5f**)*

According to the general procedure, compound **5f** was obtained by using 4-formylphenyl acetate. Yellow solid; yield 66%; HPLC purity: 96.53%; mp: 229-231℃. ^{1}H NMR (600 MHz, DMSO-d_6): δ 11.90 (br. s, 1H), 9.66 (br. s, 1H), 8.60 (d, *J*=5.5 Hz, 1H), 8.46-8.52 (m, 2H), 8.02 (d, J=8.4Hz, 2H), 7.97 (d, *J*=8.4 Hz, 1H), 7.77-7.86 (m, 3H), 7.63-7.66 (m, 1H), 7.53 (d, *J*=8.6 Hz, 2H), 7.20-7.28 (m, 2H), 7.19 (d, *J*=5.5 Hz, 1H), 2.30 (s, 3H). ^{13}C NMR (151 MHz, DMSO-d_6): δ 169.6, 163.0, 158.6, 152.1, 149.5, 148.5, 147.1, 147.0, 144.3, 144.3, 132.5, 131.0, 129.7, 128.7, 128.2, 127.8, 126.0, 123.1, 122.9, 122.9, 121.1, 120.3, 116.2, 103.6, 21.3. ESI-MS: positive mode *m/z* 425.1 $[M+H]^+$, 447.0 $[M+Na]^+$, 849.1 $[2M+H]^+$, 871.1 $[2M+Na]^+$; negative mode *m/z* 423.0 $[M-H]^-$.

*4.1.4.7. (E)-N'-(2,6-dimethoxybenzylidene)-4-(quinolin-4-ylamino)benzohydrazide (**5g**)*

According to the general procedure, compound **5g** was obtained by using 2,6-

dimethoxybenzaldehyde. Yellow solid; yield 92%; HPLC purity: 97.16%; mp: 220-223 ℃. ^{1}H NMR (600 MHz, DMSO-d6): δ 11.81 (s, 1H), 8.74 (d, J = 8.4 Hz, 1H), 8.67 (s, 1H), 8.60-8.65 (m, 1H), 8.13 (d, J = 8.3 Hz, 2H), 8.03-8.09 (m, 2H), 7.85 (ddd, J = 2.7, 5.4, 8.3 Hz, 1H), 7.63-7.68 (m, 2H), 7.33-7.40 (m, 1H), 7.03 (d, J = 6.8 Hz, 1H), 6.74 (d, J = 8.4 Hz, 2H), 3.83 (s, 6H). ^{13}C NMR (151 MHz, DMSO-d6): δ 159.2, 158.8, 158.6, 154.8, 144.2, 144.0, 140.8, 139.1, 134.5, 132.4, 131.8, 129.9, 127.7, 125.0, 123.9, 121.2, 118.0, 111.5, 104.9, 101.0, 56.5. ESI-MS: positive mode *m/z* 427.1 $[M+H]^+$, 449.3 $[M+Na]^+$,.

*4.1.4.8. (E)-N'-(3,4-dimethoxybenzylidene)-4-(quinolin-4-ylamino)benzohydrazide (**5h**)*

According to the general procedure, compound **5h** was obtained by using 3,4-dimethoxybenzaldehyde. Yellow solid; yield 84%; HPLC purity: 99.36%; mp:162-164 ℃ . ^{1}H NMR (600 MHz, DMSO-d_6): δ 11.80 (s, 1H), 8.60 (d, J = 6.1 Hz, 1H), 8.58 (d, J = 8.4 Hz, 1H), 8.42 (s, 1H), 8.05 (d, J = 8.4Hz, 2H), 8.00 (d, J = 9.0 Hz, 1H), 7.93 (t, J = 7.6 Hz, 1H), 7.74 (t, J = 7.5 Hz, 1H), 7.58 (d, J = 8.4 Hz, 2H), 7.37 (s, 1H), 7.22 (d, J = 7.5 Hz, 1H), 7.11 (d, J = 6.1 Hz, 1H), 7.05 (d, J = 8.3 Hz, 1H), 3.84 (s, 3H), 3.82 (s, 3H)^{13}C NMR (151 MHz, DMSO-d_6): δ 162.7, 161.6, 158.3, 151.2, 149.6, 148.4, 147.1, 142.7, 136.7, 132.5, 130.2, 129.7, 127.5, 126.8, 123.4, 122.9, 122.4, 119.3, 112.0, 108.7, 102.4, 56.1, 55.9 ESI-MS: positive mode *m/z* 427.1 $[M+H]^+$, 875.1 $[2M+Na]^+$.

*4.1.4.9. (E)-N'-(3,4-dihydroxybenzylidene)-4-(quinolin-4-ylamino)benzohydrazide (**5i**)*

According to the general procedure, compound **5i** was obtained by using 3,4-dihydroxybenzaldehyde. Yellow solid; yield 63%; HPLC purity: 94.89%; mp: 196-198℃. ^{1}H NMR (600 MHz, DMSO-d_6): δ 11.74 (s, 1H), 10.91 (br. s, 1H), 9.46 (br. s, 1H), 9.31 (br. s, 1H), 8.73 (d, J=8.4 Hz, 1H), 8.63 (d, J=6.8 Hz, 1H), 8.31 (s, 1H), 8.11 (d, J=8.4 Hz, 2H), 8.03-8.07 (m, 2H), 7.86 (ddd, J=1.6, 6.6, 8.4 Hz, 1H), 7.65 (d, J=8.4 Hz, 2H), 7.26 (d, J=1.7 Hz, 1H), 7.01-7.04 (m, 1H), 6.96 (dd, J=1.7, 8.1 Hz, 1H), 6.81 (d, J=7.9 Hz, 1H). ^{13}C NMR (151 MHz, DMSO-d_6): δ 162.4, 158.7, 154.8, 149.1, 148.6, 146.2, 143.9, 140.8, 139.0, 134.5, 132.4, 129.8(2C), 127.8, 126.2, 125.0(2C), 123.9, 121.1(2C), 118.0, 116.1, 113.2, 101.0. ESI-MS: positive mode *m/z* 399.1 $[M+H]^+$, 421.1$[M+Na]^+$; negative mode *m/z* 355.0 $[M-H]^-$.

*4.1.4.10. (E)-N'-(2,5-dihydroxybenzylidene)-4-(quinolin-4-ylamino)benzohydrazide (**5j**)*

According to the general procedure, compound **5j** was obtained by using 2,5-dihydroxybenzaldehyde. Yellow solid; yield 82%; HPLC purity: 98.80%; mp: 245-247 ℃. ^{1}H NMR (600 MHz, DMSO-d_6): δ 12.12 (s, 1H), 10.46 (s, 1H), 9.07 (br. s., 1H), 8.65 (d, *J* = 8.4 Hz, 1H), 8.61-8.64 (m, 2H), 8.12 (d, *J* = 8.4 Hz, 2H), 8.03-8.11 (m, 2H), 7.82-7.88 (m, 1H), 7.63 (d, *J* = 8.6 Hz, 2H), 7.09 (d, *J* = 6.8 Hz, 1H), 7.00 (d, *J* = 2.6 Hz, 1H), 6.75-6.77 (m, 2H). ^{13}C NMR (151 MHz, DMSO-d_6): δ 162.4, 158.9, 154.5, 150.7, 150.4, 148.2, 144.2, 141.3, 139.4, 134.3, 131.4, 129.9, 127.7, 124.8, 123.8, 121.5, 119.5, 118.1, 117.5, 114.2, 101.2. ESI-MS: positive mode *m/z* 399.0 $[M+H]^+$, 421.1 $[M+Na]^+$, 819.2 $[2M+Na]^+$.

4.1.4.11. (*E*)*-N'-(2-hydroxy-5-nitrobenzylidene)-4-(quinolin-4-ylamino) benzohydrazide (**5k**)*

According to the general procedure, compound **5k** was obtained by using 2-hydroxy-5-nitrobenzaldehyde. Yellow solid; yield 71%; HPLC purity: 99.40%; mp: 225-227℃. ^{1}H NMR (600 MHz, DMSO-d_6): δ 12.38 (br. s, 1H), 10.92 (br. s, 1H), 8.77-8.84 (m, 1H), 8.73 (d, *J*=8.4 Hz, 1H), 8.53-8.68 (m, 2H), 8.12-8.26 (m, 3H), 8.04-8.09 (m, 2H), 7.86 (ddd, *J*=1.3, 6.8, 8.4 Hz, 1H), 7.69 (d, *J*=8.4 Hz, 2H), 7.11-7.18 (m, 1H), 7.06 (d, *J*=6.6 Hz, 1H). ^{13}C NMR (151 MHz, DMSO-d_6): δ 163.1, 162.8, 154.7, 144.7, 144.0, 141.3, 140.4, 139.1, 134.5, 131.3, 130.0(2C), 127.8, 127.1, 125.0(2C), 123.9(2C), 121.2, 120.6, 118.1, 117.6, 101.1 ESI-MS: positive mode *m/z* 428.0 $[M+H]^+$, 450.0 $[M+Na]^+$; negative mode *m/z* 426.0 $[M-H]^-$.

4.1.4.12. (*E*)*-N'-(3,5-dibromo-4-hydroxybenzylidene)-4-(quinolin-4-ylamino) benzohydrazide (**5l**)*

According to the general procedure, compound **5l** was obtained by using 3,5-dibromo-4-hydroxybenzaldehyde. Yellow solid; yield 70%; HPLC purity: 99.40%; mp: 267-269℃. ^{1}H NMR (600 MHz, DMSO-d_6): δ 12.08 (s, 1H), 10.91 (br. s, 1H), 8.72 (d, *J*=8.4 Hz, 1H), 8.63 (d, *J*=6.8 Hz, 1H), 8.35 (s, 1H), 8.08-8.17 (m, 2H), 8.01-8.08 (m, 2H), 7.94 (s, 2H), 7.86 (ddd, *J*=1.5, 6.7, 8.3 Hz, 1H), 7.65 (s, 2H), 7.02-7.06 (m, 1H). ^{13}C NMR (151 MHz, DMSO-d_6): δ 162.8, 154.8, 152.7, 145.4, 144.0, 141.0, 139.0,

134.5, 131.9, 131.1(2C), 129.9(2C), 129.3, 127.8, 125.0(2C), 123.9, 121.1, 118.0, 112.7(2C), 101.0. ESI-MS: positive mode *m/z* 540.8 $[M+H]^+$; negative mode *m/z* 538.8 $[M-H]^-$.

*4.1.4.13. (E)-N'-((1H-imidazol-2-yl)methylene)-4-(quinolin-4-ylamino) benzohydrazide (**5m**)*

According to the general procedure, compound **5m** was obtained by using 1*H*-imidazole-2-carbaldehyde. Grey solid; yield 50%; HPLC purity: 95.32%; mp: 279-281℃. ^{1}H NMR (600 MHz, DMSO-d_6): δ 14.64 (br. s, 1H), 13.20 (br. s, 1H), 10.92 (br. s, 1H), 8.73 (d, *J*=8.4 Hz, 1H), 8.63 (d, *J*=6.8 Hz, 1H), 8.11-8.19 (m, 2H), 8.04-8.09 (m, 2H), 7.87 (ddd, *J*=1.6, 6.6, 8.4 Hz, 1H), 7.74 (d, J=8.1 Hz, 2H), 7.56-7.62 (m, 1H), 7.46-7.53 (m, 1H), 7.42 (br. s, 1H), 7.11 (d, *J*=6.8 Hz, 1H). ^{13}C NMR (151 MHz, DMSO-d_6): δ 162.9, 154.3, 144.3, 142.6, 139.6, 134.3, 131.5, 130.0(2C), 129.4, 127.7(2C), 125.2, 124.8(2C), 123.8(2C), 121.6, 118.2, 101.2. ESI-MS: positive mode *m/z* 357.0$[M+H]^+$, 379.0 $[M+Na]^+$, 713.0 $[2M+H]^+$, 735.1 $[2M+Na]^+$; negative mode *m/z* 355.0$[M-H]^-$.

*4.1.4.14. (E)-N'-((1H-pyrazol-5-yl)methylene)-4-(quinolin-4-ylamino)benzohydrazide (**5n**)*

According to the general procedure, compound **5n** was obtained by using 1*H*-pyrazole-5-carbaldehyde. Grey solid; yield 52%; HPLC purity: 92.85%; mp : 203-205℃. ^{1}H NMR (600 MHz, DMSO-d_6): δ 13.96 (br. s, 1H), 13.52 (br. s, 1H), 10.95 (br. s, 1H), 8.73 (d, *J*=8.4 Hz, 1H), 8.63 (d, *J*=6.8 Hz, 1H), 8.12 (d, *J*=7.4 Hz, 2H), 8.07 (br. s, 2H), 8.04 (br. s, 1H), 7.86 (ddd, *J*=2.6, 5.6, 8.2 Hz, 1H), 7.67-7.76 (m, 3H), 7.09 (d, *J*=6.8 Hz, 1H), 6.76 (br. s, 1H) . ^{13}C NMR (151 MHz, DMSO-d_6): δ 162.7, 154.8, 143.9, 140.9, 139.0, 134.5, 132.1, 130.7, 130.1, 129.8(2C), 127.8(2C), 125.4, 125.1(2C), 123.9, 121.1, 118.1, 101.0. ESI-MS: positive mode *m/z* 357.1 $[M+H]^+$, 379.0 $[M+Na]^+$, 713.1 $[2M+H]^+$, 735.1 $[2M+Na]^+$; negative mode *m/z* 355.0 $[M-H]^-$.

*4.1.4.15. (E)-N'-((4-methylthiazol-5-yl)methylene)-4-(quinolin-4-ylamino) benzohydrazide (**5o**)*

According to the general procedure, compound **5o** was obtained by using 4-methylthiazole-5-carbaldehyde. Yellow solid; yield 68%; HPLC purity: 98.12%; mp: 250-252℃. ^{1}H NMR (600 MHz, DMSO-d_6): δ 12.07 (s, 1H), 10.86-11.00 (m, 1H), 9.06-9.13 (m, 1H), 8.79-8.83 (m, 1H), 8.71-8.75 (m, 1H), 8.61-8.66 (m, 1H), 8.10-8.14 (m, 2H), 8.04-8.08 (m, 2H), 7.84-7.88 (m, 1H), 7.66-7.69 (m, 2H), 7.04-7.06 (m, 1H), 2.52-2.54 (m, 3H). ^{13}C NMR (151 MHz, DMSO-d_6): δ 162.5, 158.8, 155.5, 154.8, 143.9, 141.5, 141.1, 139.1, 134.5, 131.8, 129.8(2C), 128.1, 127.8, 125.0(2C), 123.9, 121.1, 118.0, 101.1, 15.8. ESI-MS: positive mode *m/z* 388.1 $[M+H]^+$, 410.0 $[M+Na]^+$, 797.0 $[2M+Na]^+$.

*4.1.4.16. (E)-N'-((1H-benzo[d]imidazol-2-yl)methylene)-4-(quinolin-4-ylamino) benzohydrazide (**5p**)*

According to the general procedure, compound **5p** was obtained by using 1*H*-benzo[*d*]imidazole-2-carbaldehyde. Yellow solid; yield 72%; HPLC purity: 94.47%; mp: 330-332℃. ^{1}H NMR (600 MHz, DMSO-d_6): δ 15.08 (br. s, 1H), 13.54 (br. s, 1H), 10.92 (br. s, 1H), 8.75 (d, *J*=8.6 Hz, 1H), 8.66 (d, *J*=6.8 Hz, 1H), 8.19-8.30 (m, 2H), 8.06-8.09 (m, 2H), 7.90-7.95 (m, 1H), 7.83-7.89 (m, 2H), 7.83 (br. s, 2H), 7.71 (d, *J*=7.9 Hz, 1H), 7.41-7.46 (m, 1H), 7.35-7.41 (m, 1H), 7.19 (d, *J*=5.9 Hz, 1H). ^{13}C NMR (151 MHz, DMSO-d_6): δ 163.1, 154.5, 148.4, 144.2, 141.5, 139.8, 139.5, 139.4, 134.4, 131.3, 130.1(2C), 127.7, 125.3, 124.9(3C), 123.9(2C), 123.4, 121.5, 121.4, 118.2, 101.2. ESI-MS: positive mode *m/z* 407.1 $[M+H]^+$, 429.0 $[M+Na]^+$, 835.1 $[2M+Na]^+$; negative mode *m/z* 405.0 $[M-H]^-$.

4.2. Biological activity

4.2.1. Cell lines and reagents.

The human hepatocellular carcinoma cell line HepG2 was purchased from the American Type Culture Collection (Manassas, VA, USA). The other two human hepatocellular carcinoma cell lines (SMMC-7721 and Huh7) and two human normal cell lines (LO2 and MRC-5) were purchased from the American type culture collection (ATCC, Shanghai China). Cells were maintained in DMEM at 37˚C with 5% CO_2 and

10% fetal bovine serum (FBS) (from Gibco, Waltham, MA, USA). The primary antibodies of α-Tubulin (T6199, Sigma-Aldrich), c-Myc (Abcam, ab39688), PARP(Cell Signaling Technology, #9542), Bcl-2 (60178-1-Ig, Protein tech), Bax (60267-1-Ig, Protein tech) and tubulin (10094-1-AP, Protein Tech). Goat and anti-rabbit secondary antibodies were obtained from Thermo Fisher Scientific, Inc.

4.2.2. RT-qPCR.

HepG2 cells were treated with **5h** and **5j** at different concentrations as indicated. 24hours after treatment, total RNA from HepG2 was isolated using TRIzol® reagent (Life technologies ambion, Inc.). qPCR was conducted using the Hieff™ qPCR SYBR® Green Master Mix (YEASEN, Inc.) and the StepOnePlus Real-Time PCR system (Applied Biosystems; Thermo Fisher Scientific, Inc.). The conditions of PCR were listed as follows: 95˚C for 5 min, then following 40 cycles of 95˚C for 10 sec, 56˚C for 30 sec, 72˚C for 20 sec, 95˚C for 15 sec. Expression levels were normalized to that of GAPDH; the relative gene expression was determined using the $2^{-\Delta\Delta Ct}$ method. Primers were synthesized by Sangon Biotech (Shanghai, China) and were presented in Table 3.

Insert Table 2 here.

Table 2. Reverse transcription-quantitative polymerase chain reaction primer sequences.

4.2.3. Western blotting

HepG2 cells were lysed with whole-cell lysis buffer containing PMSF to extract total proteins after indicated drug treatment. Equal amounts of proteins were separated via 10% polyacrylamide gel electrophoresis, and proteins were transferred onto polvinylidene difluoride (PVDF) membranes. Blocking was performed in Tris-buffered saline and 0.05% Tween-20 containing 5% nonfat milk for 1 h at 37˚C. The PVDF membranes were washed with TBST three times, then incubated with rabbit polyclonal

primary antibodies at 4˚C overnight. Subsequently, the membrane was incubated with secondary antibodies (1:10,000) for 2 h at 37˚C. Lastly, an enhanced chemiluminescence kit (Advansta, lnc.) was used to analyze the membranes according to the instruction of the manufacturer. Protein bands were scanned with Molecular Imager® ChemiDoc™ XRS+ Imaging System (Bio-Rad Laboratories, Inc., Hercules, CA, USA). The optical densities of a selection of bands were detected using ImageJ (National Institutes of Health, Bethesda, MD, USA).

4.2.4. Cell proliferation.

HepG2 cells were first plated onto a 96 well plate at a density of 5,000 cells/100 μL per well and incubated overnight in an incubator at 37˚C. Following quinolone compounds (2.5, 5, 10, 20, 40 and 80 μM) or DMSO treatment for 24 hours, 20 μL MTT reagents were added to each well, and cells were incubated in the dark for 4 h at 37˚C. Untreated cells served as a control. A spectrophotometer was used to measure the absorbance of the generated optical density (OD) value at 490 nm. The half-maximal inhibitory concentration (IC50) values were determined using GraphPad Prism 6 (GraphPad Software, Inc., La Jolla, CA, USA).

4.2.5. Colony formation.

HepG2 cells were seeded in 6-well plates with 1,000 cells per well, followed treatment with **5h** and **5j** at different concentrations as indicated for 7 days. Then, the cells were washed with 1×PBS, stained with a 0.5% crystal violet solution for 15 minutes at room temperature, and then washed with PBS, and photographed under a microscope.

4.2.6. Wound healing.

HepG2 cells were seeded in 6-well plates and incubated in complete medium (DMEM medium with 10% FBS) overnight. A 20 μL sterile pipette tip was scraped across the wells and cell debris was removed via washing with 1×PBS. The supernatant

was subsequently replaced with the serum-free medium. Cells were treated with **5h** and **5j** as indicated. Finally, the scratch wounds were analyzed at various time points (0, 24 and 48 h) under the microscope.

4.2.7. Flow cytometry analysis of the cell cycle.

HepG2 cells were cultured in 6-well dishes. Following attachment, cells were treated with **5h** and **5j**. Cell suspensions were harvested using trypsin at 37˚C and placed in precooled 70% ethanol for fixation at -20˚C overnight. Then, a ribozyme (50 μg/mL) and propidium iodide (50 μg/mL, PI; BD Biosciences, San Jose, CA, USA) were added to the cells, which were incubated in the dark at room temperature for 30 min. Samples were subsequently evaluated with a flow cytometer (ATTUNE NXT, Life tech, lnc.) and data were analyzed by ModFit LT 2.0 software (Verity Software House, Inc., Topsham, ME, USA).

4.2.8. Flow cytometry analysis of apoptosis.

HepG2 cells were plated in 6-well dishes. Following attachment, cells were treated with **5h** and **5j**. Cell suspensions were harvested via trypsin at 37˚C without EDTA, washed with 1×PBS, and resuspended in 250 mL binding buffer. Cell suspensions were stained with 5 μL PI and 5 μL Annexin V-fluorescein isothiocyanate solution (Yeasen, lnc.) and incubated at room temperature for 15 min in the dark. Samples were subsequently evaluated with a flow cytometer (ATTUNE NXT, Life tech, lnc.). All assays were performed in triplicate.

4.2.9. Immunofluorescence.

After adding slides to the 24-well plate, HepG2 cells were plated in dishes, and the culture was continued after **5h** and **5j** treatment. The culture solution was aspirated and washed twice with 1×PBS, 500 μL of 4% paraformaldehyde was added to each well, fixed at room temperature for 10 minutes, 500 μL of permeabilizing solution was added to each well for 30 minutes, and 300 μL of 5 mg/mL BSA was added at room

temperature four 1 hour. Add 25μL of 5 mg/mL BSA 1:100 with a primary antibody at room temperature for 3 hours or overnight, add 25 μL of 5 mg/mL BSA 1:100-500 with secondary antibody, avoid light at room temperature for 1 hour, add 4-5 μL slide mounting medium, seal the corners with nail polish, and stay away from light overnight. Finally, find the field of view and take a picture under a laser confocal microscope.

4.3. Statistical analysis.

GraphPad Prism software (version 6) or SPSS 20.0 (IBM Corp., Armonk, NY, USA) were used for statistical analysis. Data are presented as the mean ± standard deviation. All experiments were performed in triplicate. A Student's t-test, $\chi 2$ or one-way analysis of variance were used to evaluate whether statistically significant differences were present. A Bonferroni post-hoc test for multiple comparisons was also applied. $P<0.05$ was considered to indicate a statistically significant difference.

Declaration of Competing Interest

Authors have no conflict of interest to declare.

Acknowledgements

This work was supported by the National Natural Science Foundation of China (No. 81773600 and 81672955), the National Key R&D Program of China (2018YFA0107303), the Natural Science Foundation of Fujian Province of China (No. 2018J01132), and the Fundamental Research Funds for the Central Universities (No. 20720180051).

Appendix A. Supplementary material

References

[1] R.L. Siegel, K.D. Miller, A. Jemal, Cancer statistics, 2019, CA: A Cancer Journal for Clinicians 69(1) (2019) 7-34.

[2] P. Zamani, M. Matbou Riahi, A.A. Momtazi-Borojeni, K. Jamialahmadi, Gankyrin: a novel promising therapeutic target for hepatocellular carcinoma, Artif Cells Nanomed Biotechnol 46(7) (2018) 1301-1313.

[3] A.J. Kasmari, A. Welch, G. Liu, D. Leslie, T. McGarrity, T. Riley, Independent of Cirrhosis, Hepatocellular Carcinoma Risk Is Increased with Diabetes and Metabolic Syndrome, Am J Med 130(6) (2017) 746 e1-746 e7.

[4] Hamid Reza Mirzaei1, Amirhossein Sahebkar2,#, , Circulating microRNAs in hepatocellular carcinoma: potential diagnostic and prognostic biomarkers, Current Pharmaceutical Design 22 (2016) 5257-5269.

[5] M. Gary L. Davis, Jane Dempster, RN, James D. Meler, , Hepatocellular carcinoma: management of an increasingly common problem, Proc (Bayl Univ Med Cent) 21(3) (2008) 266–280.

[6] C.V. Dang, A. Le, P. Gao, MYC-induced cancer cell energy metabolism and therapeutic opportunities, Clin Cancer Res 15(21) (2009) 6479-83.

[7] M. Eilers, R.N. Eisenman, Myc's broad reach, Genes Dev 22(20) (2008) 2755-66.

[8] N. Meyer, L.Z. Penn, Reflecting on 25 years with MYC, Nat Rev Cancer 8(12) (2008) 976-90.

[9] S.Y. Peng, P.L. Lai, H.C. Hsu, Amplification of the c-myc gene in human hepatocellular carcinoma: biologic significance, J Formos Med Assoc 92(10) (1993) 866-70.

[10] Y. Zhao, W. Jian, W. Gao, Y.X. Zheng, Y.K. Wang, Z.Q. Zhou, H. Zhang, C.J. Wang, RNAi silencing of c-Myc inhibits cell migration, invasion, and proliferation in HepG2 human hepatocellular carcinoma cell line: c-Myc silencing in hepatocellular carcinoma cell, Cancer Cell Int 13(1) (2013) 23.

[11] R. Musiol, J. Jampilek, V. Buchta, L. Silva, H. Niedbala, B. Podeszwa, A. Palka, K. Majerz-Maniecka, B. Oleksyn, J. Polanski, Antifungal properties of new series of quinoline derivatives, Bioorg Med Chem 14(10) (2006) 3592-8.

[12] P. Palit, P. Paira, A. Hazra, S. Banerjee, A.D. Gupta, S.G. Dastidar, N.B. Mondal, Phase transfer catalyzed synthesis of bis-quinolines: antileishmanial activity in experimental visceral leishmaniasis and in vitro antibacterial evaluation, Eur J Med Chem 44(2) (2009) 845-53.

[13] L.J. Guo, C.X. Wei, J.H. Jia, L.M. Zhao, Z.S. Quan, Design and synthesis of 5-alkoxy-[1,2,4]triazolo[4,3-a]quinoline derivatives with anticonvulsant activity, Eur J Med Chem 44(3) (2009) 954-8.

[14] V.R. Solomon, H. Lee, Quinoline as a Privileged Scaffold in Cancer Drug Discovery, Current Medicinal Chemistry 18(10) (2011) 1488-1508.

[15] Canonici, Neratinib overcomes trastuzumab resistance in HER2 amplified breast cancer, Oncotarget 4(10) (2013).

[16] N. Tharayil, P. Bhowmik, P. Alpert, E. Walker, D. Amarasiriwardena, B. Xing, Dual purpose secondary compounds: phytotoxin of Centaurea diffusa also facilitates nutrient uptake, New Phytol 181(2) (2009) 424-434.

[17] S.H. Chan, C.H. Chui, S.W. Chan, S.H. Kok, D. Chan, M.Y. Tsoi, P.H. Leung, A.K. Lam, A.S. Chan, K.H. Lam, J.C. Tang, Synthesis of 8-hydroxyquinoline derivatives as novel antitumor agents, ACS Med Chem Lett 4(2) (2013) 170-4.

[18] I.H. Pun, D. Chan, S.H. Chan, P.Y. Chung, Y.Y. Zhou, S. Law, A.K. Lam, C.H. Chui, A.S. Chan, K.H. Lam, J.C. Tang, Anti-cancer Effects of a Novel Quinoline Derivative 83b1 on Human Esophageal Squamous Cell Carcinoma through Down-Regulation of COX-2 mRNA and PGE2, Cancer Res Treat 49(1) (2017) 219-229.

[19] W. Kemnitzer, J. Kuemmerle, S. Jiang, H.Z. Zhang, N. Sirisoma, S. Kasibhatla, C. Crogan-Grundy, B. Tseng, J. Drewe, S.X. Cai, Discovery of 1-benzoyl-3-cyanopyrrolo[1,2-a]quinolines as a new series of apoptosis inducers using a cell- and caspase-based high-throughput screening assay. Part 1: Structure-activity relationships of the 1- and 3-positions, Bioorg Med Chem Lett 18(23) (2008) 6259-64.

[20] S. Hamzehlou, M. Momeny, Z. Zandi, B. Kashani, H. Yousefi, A.R. Dehpour, J. Tavakkoly-Bazzaz, S.H. Ghaffari, Anti-tumor activity of neratinib, a pan-HER inhibitor, in gastric adenocarcinoma cells, European Journal of Pharmacology 863 (2019) 172705.

[21] P.F.M. Oliveira, B. Guidetti, A. Chamayou, C. Andre-Barres, J. Madacki, J. Kordulakova, G. Mori, B.S. Orena, L.R. Chiarelli, M.R. Pasca, C. Lherbet, C. Carayon, S. Massou, M. Baron, M. Baltas, Mechanochemical Synthesis and Biological Evaluation of Novel Isoniazid Derivatives with Potent Antitubercular Activity, Molecules 22(9) (2017).

[22] L.C. Huan, P.T. Tran, C.V. Phuong, P.H. Duc, D.T. Anh, P.T. Hai, L.T.T. Huong, N.T. Thuan, H.J. Lee, E.J. Park, J.S. Kang, N.P. Linh, T.T. Hieu, D.T.K. Oanh, S.B. Han, N.H. Nam, Novel 3,4-dihydro-4-oxoquinazoline-based acetohydrazides: Design, synthesis and evaluation of antitumor cytotoxicity and caspase activation activity, Bioorg Chem 92 (2019) 103202.

[23] L.C. Huan, C.V. Phuong, L.C. Truc, V.N. Thanh, H. Pham-The, L.T. Huong, N.T. Thuan, E.J. Park, A.Y. Ji, J.S. Kang, S.B. Han, P.T. Tran, N.H. Nam, (E)-N'-Arylidene-2-(4-oxoquinazolin-4(3H)-yl) acetohydrazides: Synthesis and evaluation of antitumor cytotoxicity and caspase activation activity, J Enzyme Inhib Med Chem 34(1) (2019) 465-478.

[24] V.T. Angelova, M. Rangelov, N. Todorova, M. Dangalov, P. Andreeva-Gateva, M. Kondeva-Burdina, V. Karabeliov, B. Shivachev, J. Tchekalarova, Discovery of novel indole-based

aroylhydrazones as anticonvulsants: Pharmacophore-based design, Bioorg Chem 90 (2019) 103028.

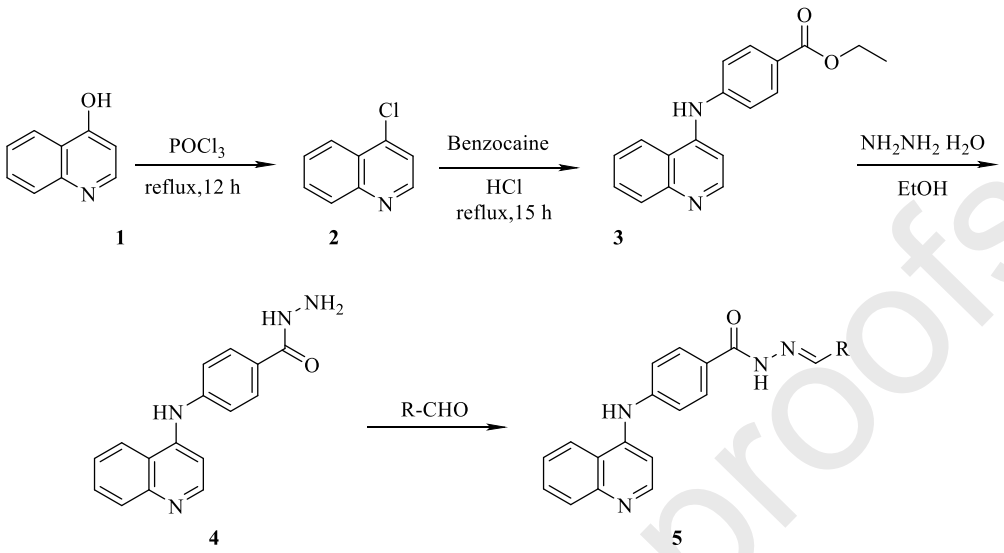

1 2 3 4 5

Compd.	R	Compd.	R	Compd.	R
5a	methyl	**5g**	2,6-dimethoxyphenyl	**5m**	1*H*-imidazole-2-yl
5b	n-propyl	**5h**	3,4-dimethoxyphenyl	**5n**	1*H*-pyrazole-5-yl
5c	2-(trifluoromethyl)phenyl	**5i**	3,4-dihydroxyphenyl	**5o**	4-methylthiazole-5-yl
5d	2-benzoic acid-1-yl	**5j**	2,5-dihydroxyphenyl	**5p**	1*H*-benzo[*d*]imidazole-2-yl
5e	3-benzoic acid-1-yl	**5k**	4-nitrophenol-2-yl		
5f	4-phenyl acetate-1-yl	**5l**	3,5-dibromo-4-hydroxyphenyl		

Scheme 1. Preparation of target compounds **5a-5p**

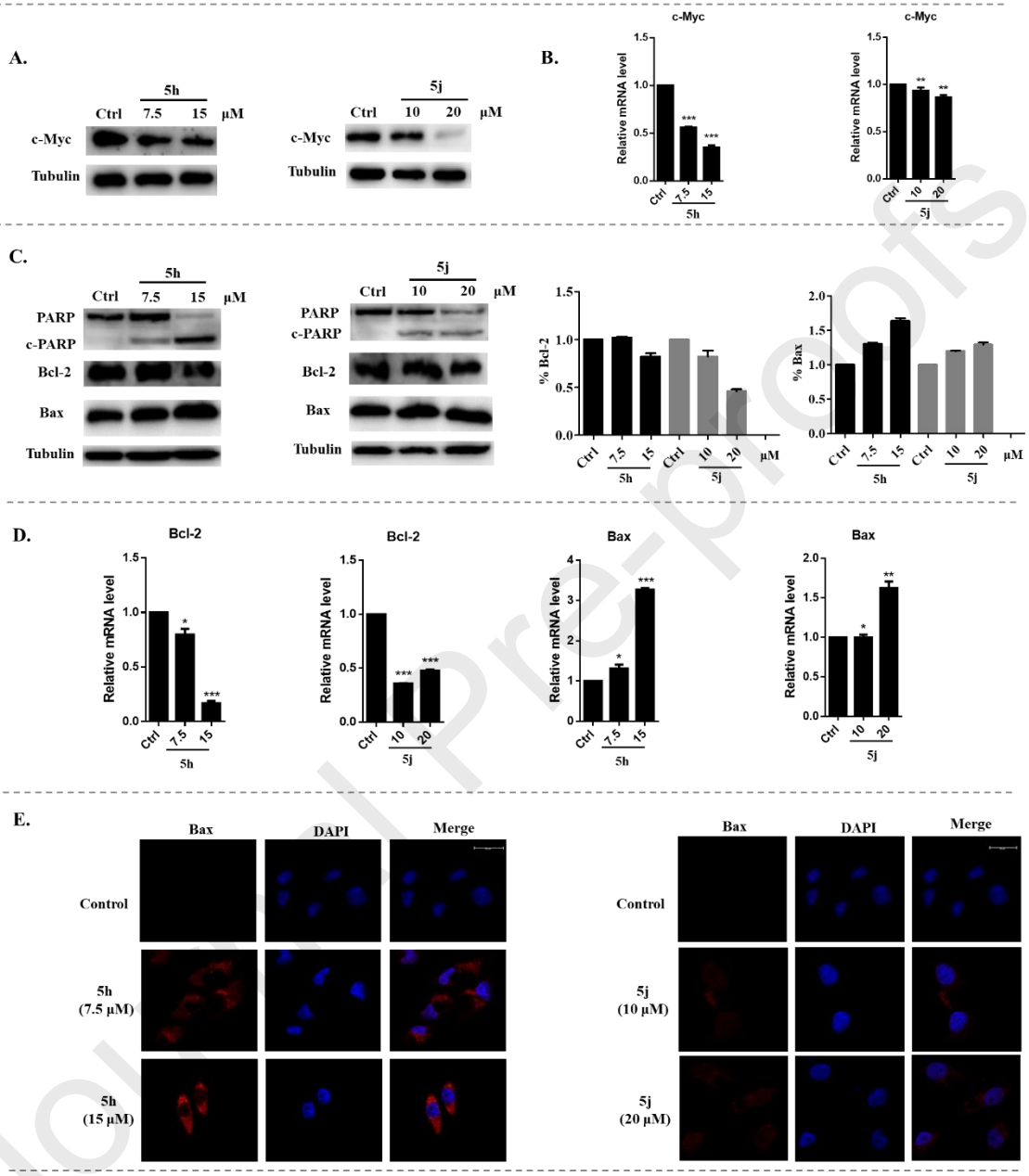

Figure 1. Modulating effect of **5h** and **5j** on the key proteins of cancer. (A). The expression level of c-Myc in HepG2 cells treated with **5h** or **5j** for 24 h, determined via Western blot. (B). mRNA level of c-Myc in HepG2 cells treated with **5h** or **5j** for 24 h determined by RT-PCR. (C). The expression level of Bcl-2, Bax, and c-PARP proteins in HepG2 cells treated with **5h** or **5j**, determined via Western blot. (D). mRNA levels of Bcl-2 and Bax in HepG2 cells treated with **5h** or **5j** for 24 h determined by RT-PCR. (E). Immunofluorometric images of Bax, DAPI staining and merge in untreated or treated HepG2 cells with **5h** and **5j** for 24 h. (∗) $P < 0.05$, (∗∗) $P < 0.01$, (∗∗∗) $P < 0.001$ compared with control group.

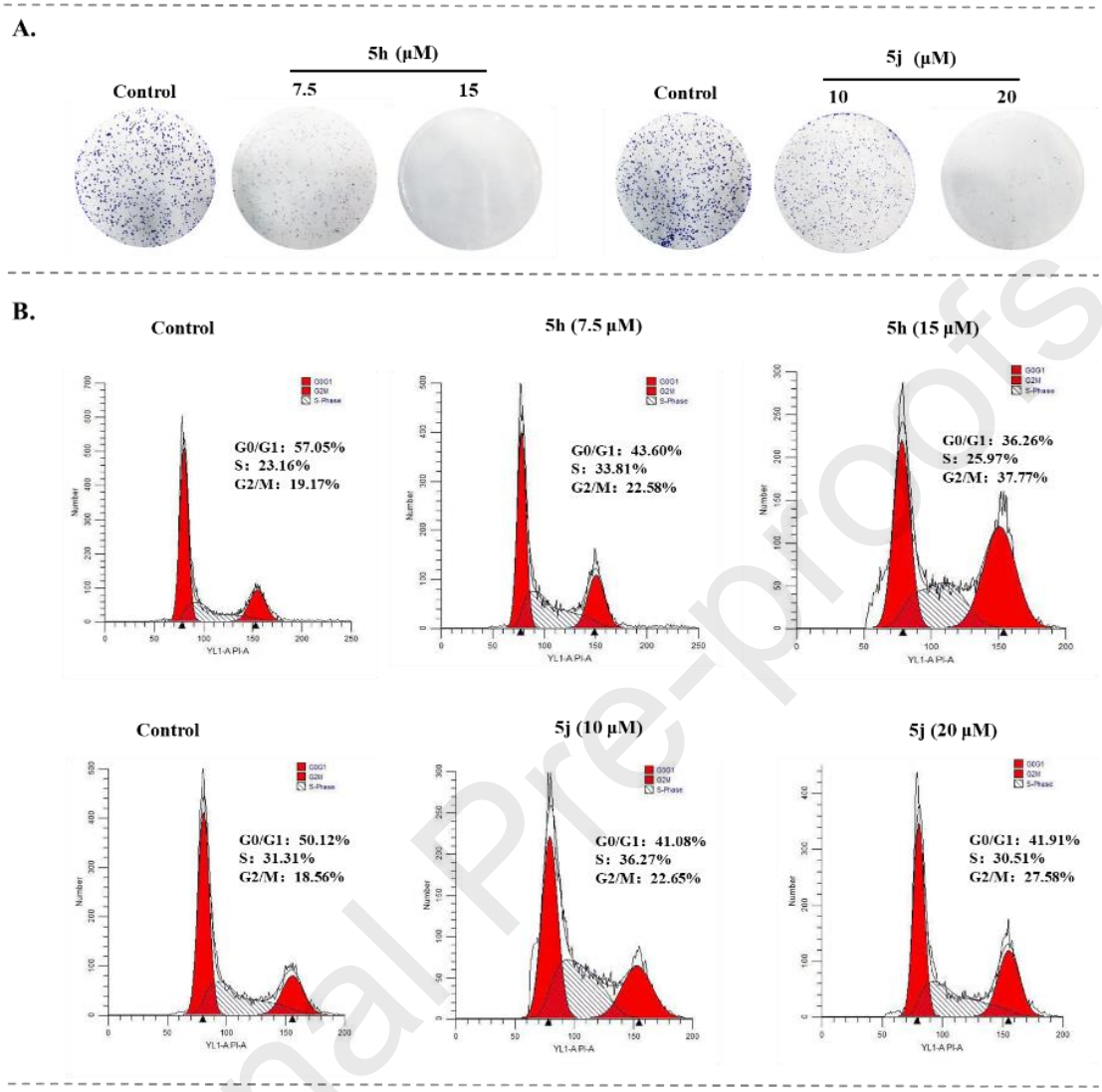

Figure 2. Cell colony formation and cell cycle phase distribution of HepG2 cells with or without treatment of compounds **5h** and **5j**. (A) Compounds **5h** or **5j** suppressed cell colony formation of HepG2 cells. HepG2 cells were incubated with varying concentrations of compounds **5h** or **5j** for 7 days and dyed with 0.1% crystal violet. (B) Compounds **5h** or **5j** induced cell cycle arrest at the G2/M phase in HepG2 cells. HepG2 cells were plated in six-well plates for 24 h and treated with or without compound **5h** and **5j** and at different concentrations for 24 h of incubation. Then, the cells were harvested to determine the PI-stained DNA content via flow cytometry.

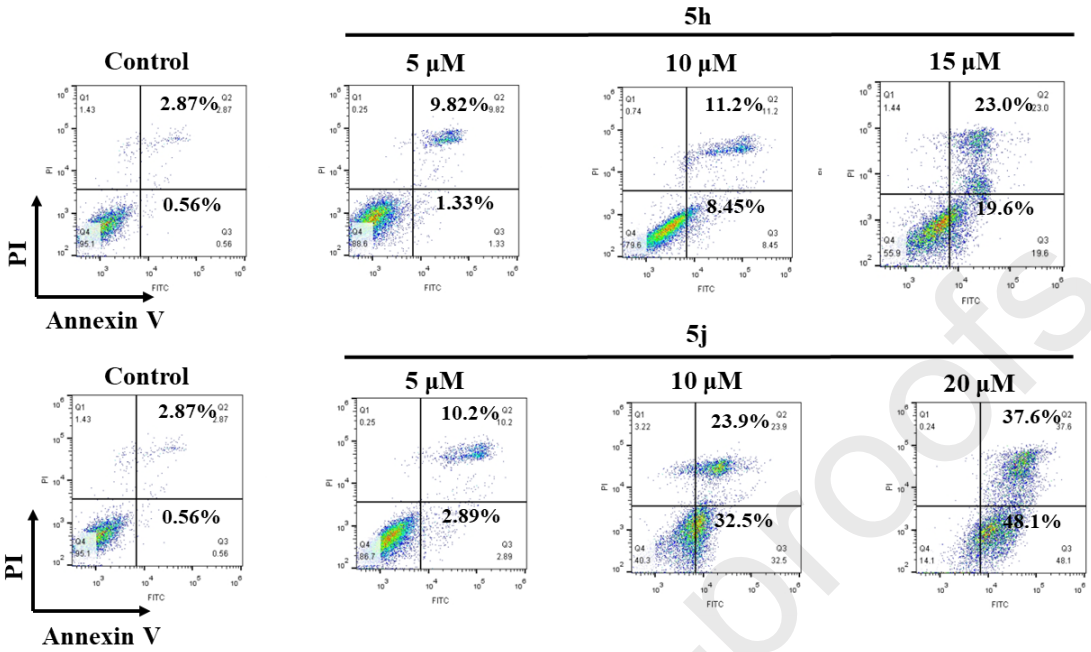

Figure 3. Apoptosis analysis of **5h** and **5j** in HepG2 cells. Cells were treated with **5h** or **5j** at distinct concentrations for 24 h, and the cell apoptosis induction of these cells was analyzed by flow cytometry.

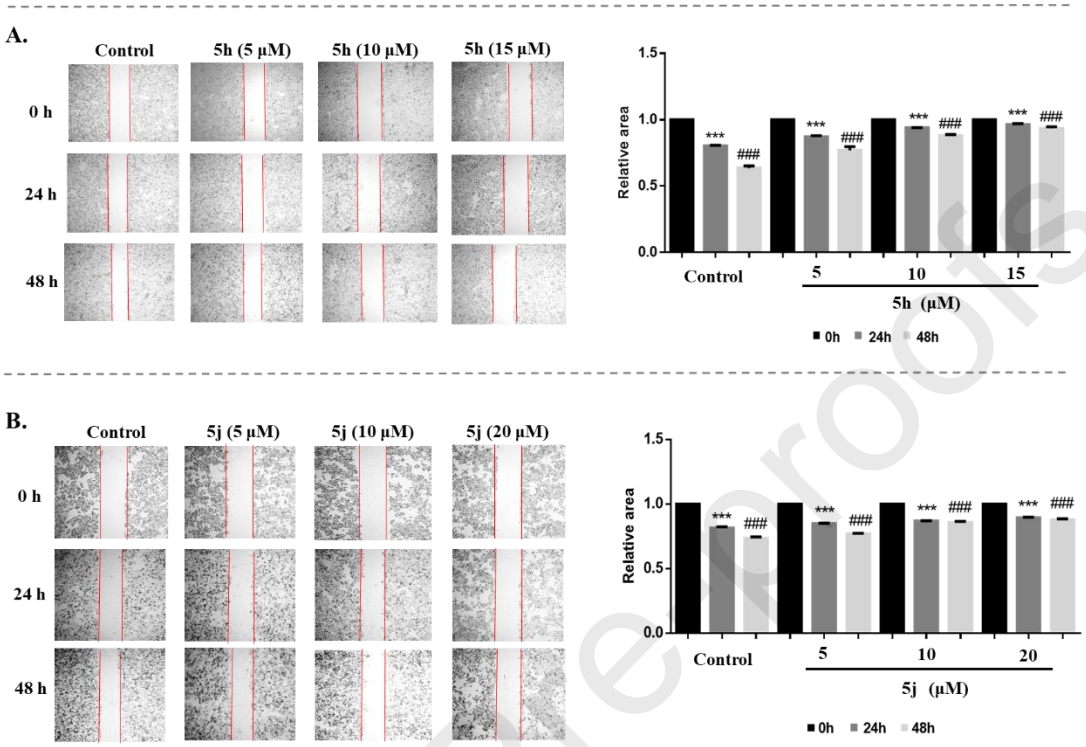

Figure 4. The effects of compounds **5h** and **5j** on the migration of HepG2 cells (A&B). Compounds **5h (A) and 5j (B)** suppressed the migration of HepG2 cells in a dose-dependent manner.

Synthesis and biological evaluations of *N'*-Substituted methylene-4-(quinoline-4-amino) benzoylhydrazides as potential anti-hepatoma agents

Baicun Li,[1, 2, #] Feifeng Zhu,[1, #] Fengming He,[1, #] Qingqing Huang,[1] Tong Wu,[1] Taige Zhao,[1] Yingkun Qiu,[1] Zhen Wu,[1] Yuhua Xue,[1, *] Meijuan Fang[1, *]

Highlights:

Novel quinoline derivatives **5h** and **5j** act as c-Myc inhibitors.

5h exhibits potent cytotoxicity against all tested human hepatic carcinoma cell lines (HepG2, SMMC-7721, and Huh7).

5h and **5j** inhibit HepG2 cell growth due to anti-survival effects, cell cycle arrest, and the induction of apoptotic cell death.

5h and **5j** suppress HepG2 cell migration.

Synthesis and biological evaluations of *N'*-Substituted methylene-4-(quinoline-4-amino) benzoylhydrazides as potential anti-hepatoma agents

Baicun Li,[1, 2, #] Feifeng Zhu,[1, #] Fengming He,[1, #] Qingqing Huang,[1] Tong Wu,[1] Taige Zhao,[1] Yingkun Qiu,[1] Zhen Wu,[1] Yuhua Xue,[1, *] Meijuan Fang[1, *]

Graphical Abstract:

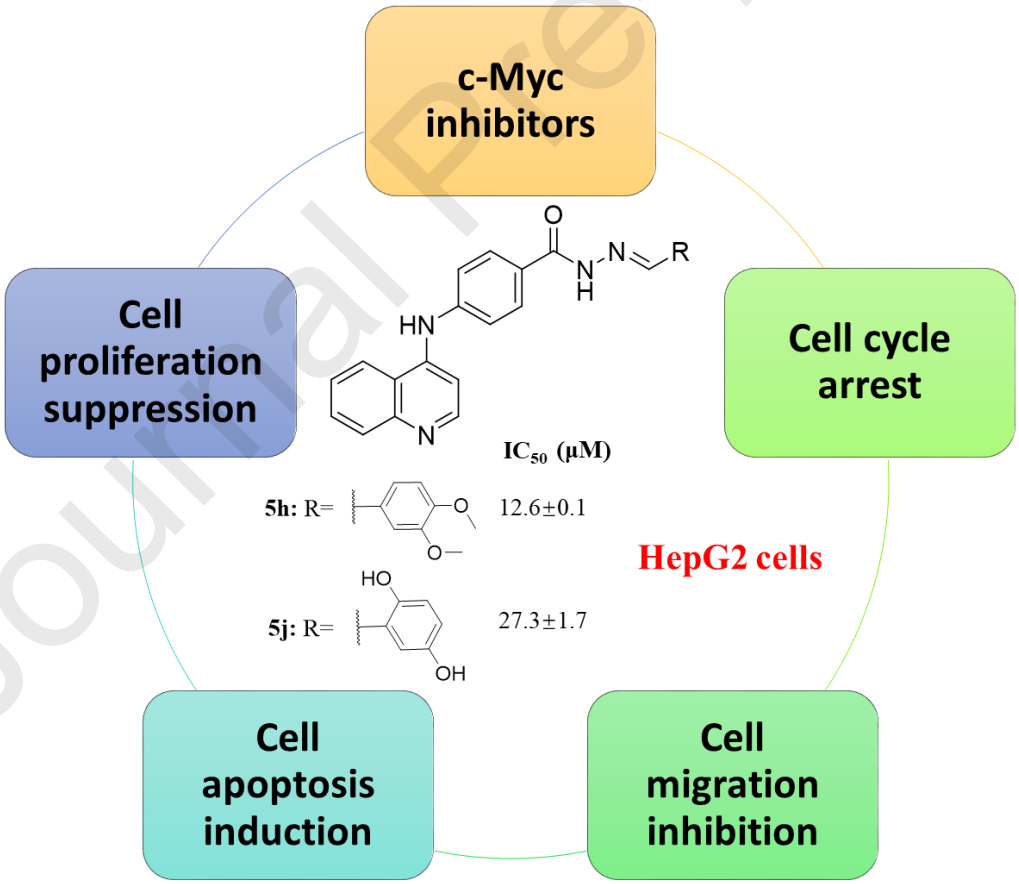

Novel quinoline derivatives **5h** and **5j** act as c-Myc inhibitors and suppress HepG2 cell growth and migration.

Table 1. *In vitro* cytotoxic activity of target compounds **5a-5p** against HepG2 cells

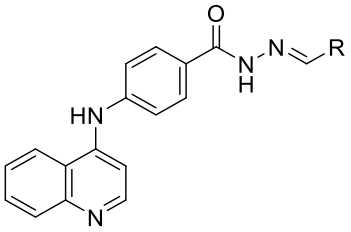

Compd.	R	IC_{50}	Compd.	R	IC_{50}
4	H	>80	**5i**	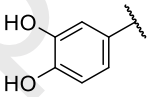	ND
5a		>80	**5j**	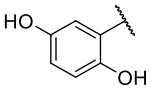	27.3±1.7
5b	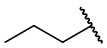	61.7±0.4	**5k**	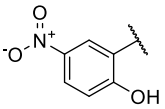	ND
5c	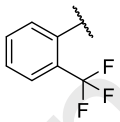	46.0±1.5	**5l**	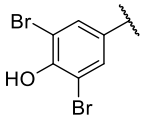	>80
5d	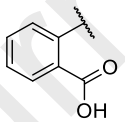	ND	**5m**		>80
5e	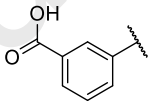	>80	**5n**	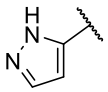	>80
5f	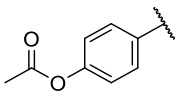	>80	**5o**	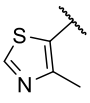	>80
5g	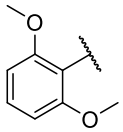	38.1±0.8	**5p**	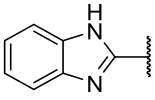	>80
5h	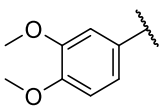	12.6±0.1	**LNTN**		5.10±0.3

Data are means ± SD of triplicate experiments. ND: no detect.

Table 2. The anti-hepatoma effect and safety of **5h** and **5j**

Compounds	Hepatic carcinoma cells			Normal cells	
	HepG2	SMMC-7721	Huh7	LO2	MRC-5
5h	12.6±0.1	9.6±0.7	6.3±0.2	16.1±1.6	30.4±3.0
5j	27.3±1.7	>50	18.6±1.5	>50	>50
LNTN	5.10±0.3	9.64±0.4	5.9±0.5	19.1±2.5	29.6±1.6

Data are means ± SD of triplicate experiments.

Table 3. Reverse transcription-quantitative polymerase chain reaction primer sequences.

Gene	Forward (5'-3')	Reverse (5'-3')
c-Myc	CCCTCCACTCGGAAGGACTA	GCTGGTGCATTTTCGGTTGT
Bax	CCCGAGAGGTCTTTTTCCGAG	CCAGCCCATGATGGTTCTGAT
Bcl-2	ATGTGTGTGGAGAGCGTCAA	ACAGTTCCACAAAGGCATCC
GAPDH	GCACCACCAACTGCTTAGC	GGCATGGACTGTGGTCATG

Declaration of Competing Interest

Authors have no conflict of interest to declare.